FOPID controller based AGC loop of a two-area Solar-Thermal deregulated Power System with Vanadium Redox Flow Battery

B. Baskar, Lecturer, Department of EEE, Government Polytechnic College, Sankarapuram, Tamilnadu, India, baskar.prb@gmail.com

B. Paramasivam, Assistant Professor, Department of EEE, Government College of Engineering, Bodinayakkanur, Tamilnadu, India, bpssivam@gmail.com

Abstract - This paper presents Automatic Generation Control (AGC) of an interconnected two-area solar-thermal deregulated power system considering Vanadium Redox Flow Batteries (VRFB). The conventional AGC loop may never again have the capacity to constrict the extensive frequency oscillation because of the moderate reaction of the governor for unusual load variations. In VRFB unit having capacity limit notwithstanding the kinetic energy of the generator rotors is fitting to sodden out the frequency oscillations. The execution of VRFB catches the fundamental fall in frequency and also the tie-line power deviations after an unexpected load agitating impact. Another fractional-order proportional-integral-derivative (FOPID) controller is proposed as strengthening control for AGC loop. The tuning of the FOPID controller parameters is formulated as an optimization problem and explained by utilizing a Lightning Search Algorithm (LSA). Simulation reveals that the proposed FOPID controller tuned with LSA algorithm liven up the dynamic output response of the test system to the extent less apex deviation and settling time of area frequencies and tie-line power oscillations in different trades of the deregulated power system. Besides, the Power stream control by VRFB unit is likewise observed to be productive and successful for improving the dynamic performance of the AGC loop interconnected power system.

Keywords — Automatic Generation Control, Deregulated Power System, FOPID controller, Lightning Search Algorithm, Solar Thermal Power Plant, Vanadium Redox Flow Batteries.

I. INTRODUCTION

In current power system network there are number of generating utilities interconnected together through tie-lines. With a specific end goal to accomplish coordinated task of a power system, an electric energy system must be kept up at a coveted working level portrayed by ostensible frequency, voltage profile and load flow configuration. Right now the regular power system has been changed to deregulated condition. A deregulated power system includes generation companies (Gencos), distribution companies (Discos), transmission companies (Transco) and Independent System Operator (ISO). The deregulated power system, Automatic Generation Control (AGC) is the essential control issue in an interconnected power system. The most imperative goals of the AGC is to keep up system frequency and tie-line power deviations within permissible limit by directing the output power of every generator at concurred levels in light of persistently changing load demand [1]. The AGC activity is coordinated by the Area Control Error (ACE) which is a job of system frequency and tie line power flows. As the ACE is engaged to zero by the AGC both recurrence and tie-line control blunders will be put on to zero [2]. An ISO is a self-overseeing specialist that deals with every one of the exchanges accepted among Discos and Gencos. A Disco Participation Matrix (DPM) is utilized for the pipedream of bonds among Gencos and Discos [3]. An ISO needs to perform different auxiliary administrations for winning activity of the power system [4]. Because of carbon emanation issues and quickly diminishing traditional energy resources, there is a need to locate some elective sources so future energy demands can be met. Solar energy and wind energy sources are such choices. Solar energy has large potential and according to recent studies, it has potential to be energy source of future. The fundamental ideas of displaying and joining of sustainable power sources in the power system have been presented in literature [5-7]. The idea of the mix of solar-thermal power plant (STPP) for AGC ponders be that as it may, their investigation is confined to a detached system just and they have not connected any control methodology for STPP [8]. The solar energy is a spotless energy accessible in copious. Conversion of solar energy into electric energy does not discharge ozone-depleting substances. Additionally, the utilization of this

 DOI : 10.18231/2454-9150.2019.0134

nonconventional energy diminishes the utilization of regular well springs of energy. Till now, no study on AGC in multi area system incorporating STPP is available in the literature. Hence, AGC of multi-area system incorporating solar thermal power plant (STPP) is important for further studies.

Energy storage devices, for example, Capacitive Energy Storage (CES), Superconductor Magnetic Energy Storage Systems (SMES) and Vanadium Redox Flow Batteries (VRFB) have enhanced the power exchange ability and power administration of the interconnected power system. Vanadium Redox Flow Batteries (VRFB) is a vigorous power source which can be vital not just as a quick energy compensation device for power use of gigantic loads yet additionally as a stabilizer of frequency oscillations [9]. The VRFB have been remunerated an amassing of load and could keep up power quality for deregulated control supplies. In any case, because of the monetary rationale, it isn't practical to rest VRFB in every area. The VRFB have been compensate an accumulation of load and could be maintain power quality for deregulated power supplies. But, due to the economical motive it is not feasible to rest RFB in each area frequency oscillations.

Then again, for the optional control of AGC, a few traditional controller structures, for example, integral (I), Proportional-Integral (PI), Proportional-Integral-Derivative (PID), and Integral Derivative (ID) have been utilized and their execution has been looked at for an AGC system and it is set up that PID controller give better execution over alternate controllers [10]. Be that as it may, the primary detriments of the parallel PID controllers are the belonging of proportional and derivative kick, which grades in abrupt spikes and gratuitous overshoot. In a PID controller, the derivative mode recoups steadiness of the system and improves the speed of the controller response yet it makes the plant to draw a colossal measure of control input. Additionally, any noise in the control input signal will in large plant input signals distortion which often leads to complications in practical applications.

The practical solution to these problems is to put a first filter on the imitative term and tune its pole so that the distortion due to the noise does not occur since it eases high frequency noise [11]. The performance of PID controllers can be improved by using the fractional calculus. In fractional order (FO) controllers, the order of integral and derivative terms is not an integer [12]. The main advantage associated with FO controllers is flexibility in controlling purpose which helps to design a robust control system. FO controllers have excellent capability of handling parameter uncertainty, elimination of steady state error and better stability [13]. Fractional order proportional integral derivative (FOPID) controllers are being used in different fields of engineering, such as stabilizing fractional order time delay systems, automatic voltage regulator system, etc.

Several optimization techniques plays an important role to find the optimal controller parameters, for example, Genetic Algorithm (GA), Particle Swarm Optimization (PSO), Bacterial Foraging Optimization (BFO), Krill Herd Algorithm (KHA), and Teaching Learning Based Optimization (TLBO)) algorithm have been planned to resolve the control parameters of a several standard controllers to solve the AGC problem [14-17]. A later intense meta-heuristic algorithm called Lightning Search Algorithm (LSA) is a great and adaptable advancement strategy that was propelled by the characteristic wonder of lightning [18, 19]. The advantages of this algorithm are to be used for optimization of PI, PID, and FOPID controller gains of AGC loop for two-area solar-thermal interconnected deregulated power system without and with VRFB units for different transactions.

II. MODELING OF TWO-AREA SOLAR-THERMAL POWER SYSTEM WITH REHEAT TANDEM COMPOUND STEAM TURBINE IN DEREGULATED ENVIRONMENT

In the deregulated power system, Discos in each zone can bond with Gencos in its own or different zones. There are a few Gencos and Discos in the deregulated power system; a Disco has the freedom to have an agreement with any Genco for the agreement of power. Such exchanges are called bilateral exchanges [3]. Every one of the exchanges must be cleared through a fair element called an ISO. In this two-area solar-thermal power system is considered in which every territory has two Gencos and two Discos is appeared in Fig 1. The AGC execution is acknowledged on the steam turbine dynamic model parameters. The steam turbine show parameters are observed to be dependent on the generation schedules of thermal power plants [20]. The dynamic models of reheat bicycle mix condensation turbine are appeared in Fig 2. The principle requirements of these models are the time constants T_{SC}, T_{RH} and T_{CO} of Steam Chest (SC), Reheater (RH) and Cross-Over (CO) pipe respectively and the power divisions F_{HP}, F_{IP} and F_{LP} of High Pressure (HP), Intermediate-Pressure (IP) and Low Pressure (LP) turbines separately. The regular estimations of different time constants and power bits of thermal reheat turbine can be intended for various generation schedules by expelling the heat balance data is appeared in the appendix.

 DOI : 10.18231/2454-9150.2019.0134

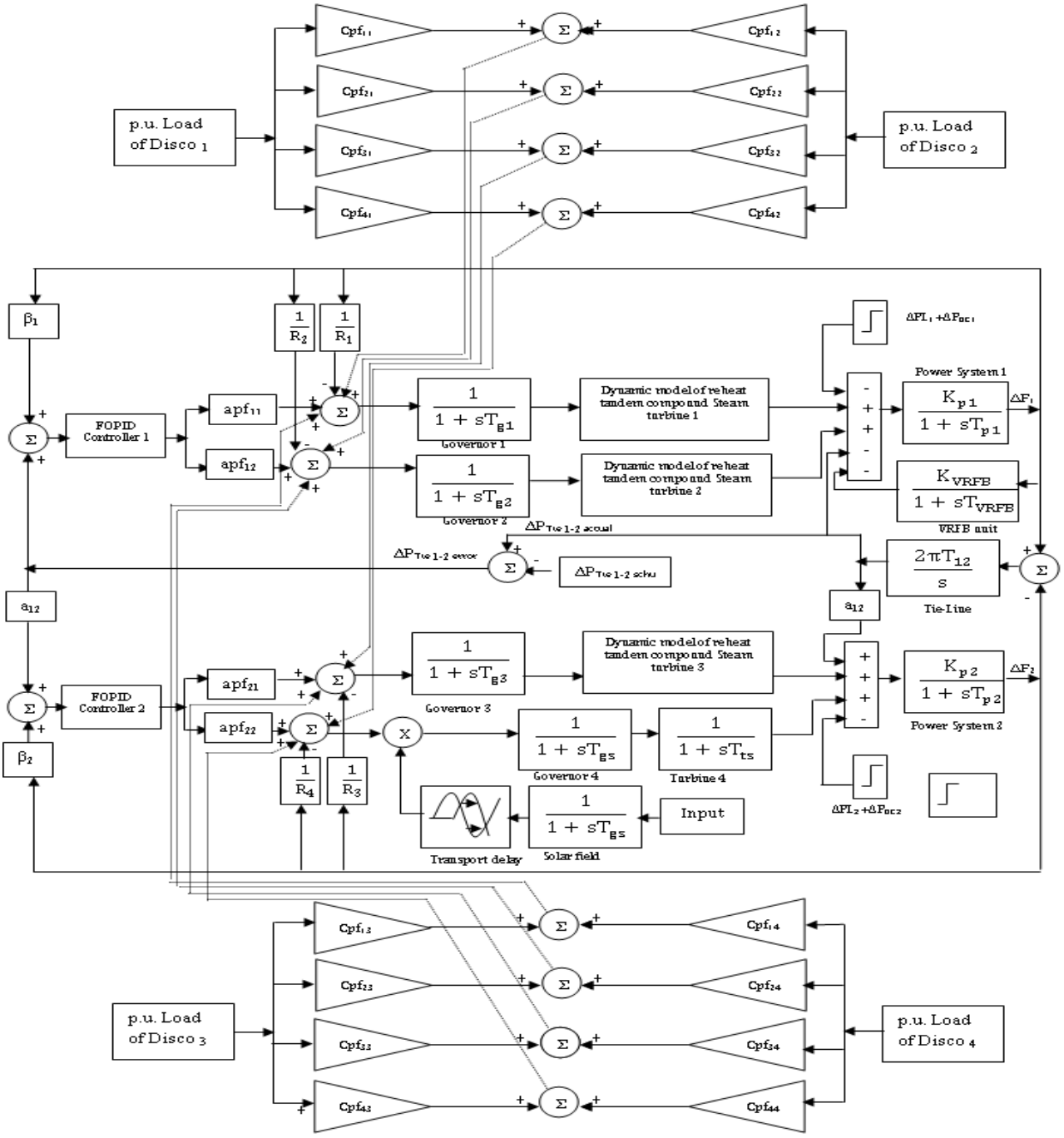

Fig.1 Transfer function model of two area solar-thermal power system with VRFB unit in deregulated environment

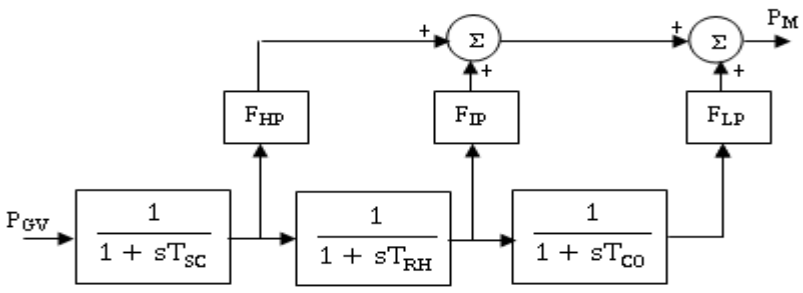

Fig.2 Dynamic model of a reheat tandem compound steam turbine

In the new environment, Discos may contract power from any Gencos and ISO has to supervise these contracts. DPM is a matrix in which the number of rows is equal to the number of Gencos and the number of columns is equal to the number of Discos in the system each entry in this matrix can be considered for the portion of a total load contracted by a Disco towards a Genco. The sum of all the entries in a column DPM is unity. From the Fig 1, Let Genco1,

 DOI : 10.18231/2454-9150.2019.0134

Genco2, Disco1, Disco2 be in area 1 and Genco3, Genco4, Disco3, Disco4 be in area 2. The corresponding DPM is given as follows

$$DPM = \begin{bmatrix} cpf_{11} & cpf_{12} & cpf_{13} & cpf_{14} \\ cpf_{21} & cpf_{22} & cpf_{23} & cpf_{24} \\ cpf_{31} & cpf_{32} & cpf_{33} & cpf_{34} \\ cpf_{41} & cpf_{42} & cpf_{43} & cpf_{44} \end{bmatrix} \quad (1)$$

where *cpf* represents "contract participation factor" i.e. p.u. MW load of a corresponding Disco. The scheduled steady state power flow on the tie-line is given as [3]

$$\Delta P_{Tie\ 12}^{scheduled} = \sum_{i=1}^{2}\sum_{j=3}^{4} cpf_{ij}\,\Delta P_{Lj} - \sum_{i=3}^{4}\sum_{j=1}^{2} cpf_{ij}\,\Delta P_{Lj} \quad (2)$$

The actual tie-line power is given as

$$\Delta P_{Tie\ 12}^{actual} = \frac{2\pi T_{12}}{s}(\Delta F_1 - \Delta F_2) \quad (3)$$

At any given time, the tie-line power error is given by [3]

$$\Delta P_{Tie\ 12}^{Error} = \Delta P_{Tie\ 12}^{actual} - \Delta P_{Tie\ 12}^{scheduled} \quad (4)$$

$\Delta P_{Tie\ 12}^{Error}$, vanishes in the steady as the actual tie-line power flow reaches the scheduled power flow. This error signal is used to generate the respective Area Control Error (ACE) signals as in the traditional scenario [3].

$$ACE_1 = \beta_1 \Delta F_1 + \Delta P_{Tie12}^{Error} \quad (5)$$

$$ACE_2 = \beta_2 \Delta F_2 + a_{12}\Delta P_{Tie12}^{Error} \quad (6)$$

The generation of each Genco must footpath the contracted demands of Discos in steady state. The desire total power generation of i[th] Genco in terms of DPM entries can be calculated as

$$\Delta P_{mi} = \sum_{j=1}^{4} cpf_{ij}\,\Delta P_{Lj} \quad (7)$$

As there are two Gencos in every area, the ACE signal must be scattered among them in proportion to their participation in the AGC. Coefficients that circulate ACE to Gencos are named as ""ACE Participation Factors (apfs)". In a given control territory, the entirety of the participation factors is equal to 1. Consequently, apf_{11}, apf_{12} are considered as ACE participation factor in area 1 and apf_{21}, apf_{22} are in area 2.

III. DESIGN OF FOPID CONTROLLER USING LIGHTNING SEARCH ALGORITHM

3.1 Controller structure of FOPID controller

The block diagram of Fractional Order PID (FOPID) controller, referred to as $PI^{\lambda}D^{\mu}$ controller is shown in Fig.3. In FOPID controller, in addition to K_P, K_I and K_D there are two more parameters λ and μ, the integral and derivative orders respectively. The transfer function of proposed FOPID controller is given by

$$T(s) = K_P + \frac{K_I}{s^{\lambda}} + K_D s^{\mu} \qquad \lambda, \mu > 0 \quad (8)$$

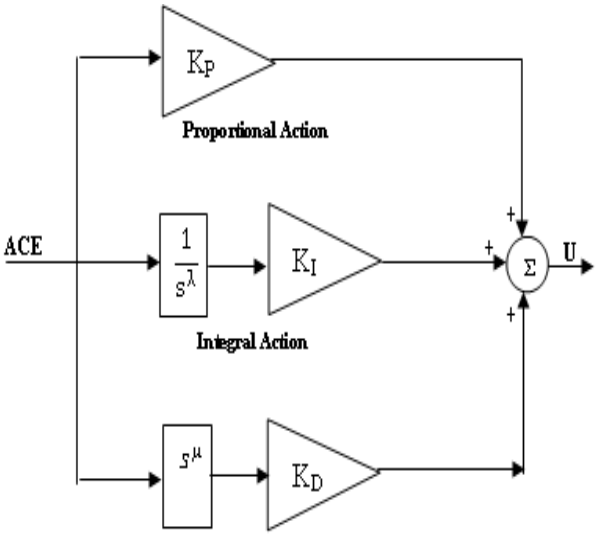

Fig. 3 Block diagram for FOPID controller

On the off chance that λ=0 and μ=0, at that point it is simply just a proportional (P) controller, If λ=0 and μ=1, at that point it turns into a proportional-derivative (PD) controller, If λ=1 and μ=0, at that point it turns into a proportional-integral (PI) controller and If λ=1 and μ=1, at that point it moves toward becoming whole number PID. These whole number request controllers are spoken to as focuses in the λ-μ plane as appeared in Fig. 4 (a). Accordingly FOPID controller sums up the PID controller and extends it from point to whole λ-μ plane as appeared in Fig. 4 (b) hence offering the significantly more extensive determination of tuning parameters subsequently greater adaptability in the controller configuration prompting more exact control [13]. The LSA methods are utilized to decide the ideal requirements of PI, PID and FOPID controllers with the target to limit the Integral square of area control error, which can be defined in the accompanying way:

$$J = \int_0^{t_{sim}} (\beta_1 \Delta F_1^2 + \beta_2 \Delta F_2^2 + \Delta P_{tie}^2)\, dt \quad (9)$$

The problem constraints are the proposed controller parameter bounds. Therefore, the design problem can be formulated as,

$$Minimize\ J \quad (10)$$

Subject to

$$K_P^{min} \le K_P \le K_P^{max}, K_I^{min} \le K_I \le K_I^{max}, K_D^{min} \le K_D \le K_D^{max}, K_{FR}^{min} \le K_{FR} \le K_{FR}^{max}, N^{min} \le N \le N^{max}, \lambda^{min} \le \lambda \le \lambda^{max}, \mu^{min} \le \mu \le \mu^{max}, \quad (11)$$

 DOI : 10.18231/2454-9150.2019.0134

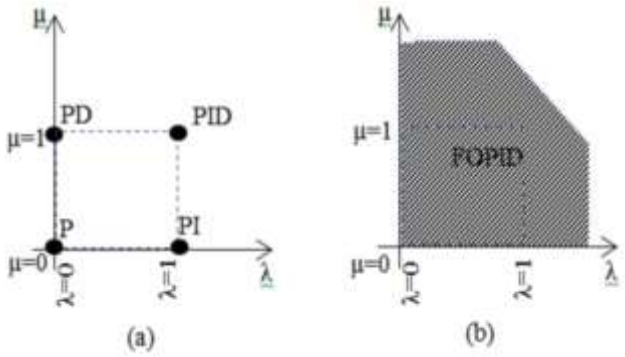

Fig. 4(a) Integer order P/PI/PD/PID controllers (b) Fractional order PID controller

3.2 Lightning Search Algorithm

LSA is a characteristic wonder in light of a novel meta-heuristic calculation. It depends on the lightning instrument which includes the proliferation of step pioneer [18, 19]. A portion of the atoms of water dense from a thundercloud split in irregular ways, known as projectile. It is viewed as that the quick particles called projectile frame the paired tree structure of the progression pioneer. The underlying populace size of the calculation is spoken to by these shots. The velocity of the projectile is appeared in (12)

$$v_p = \left[1 - \left(\frac{1}{\sqrt{1-\left(\frac{v_0}{c}\right)^2 - \left(\frac{sF_i}{mc^2}\right)}}\right)^{-2}\right]^{-1/2} \quad (12)$$

Where v0 is the underlying velocity of the projectile, m is the mass of the projectile, Fi is the steady ionization rate, c is the speed of light and s is the length of the way voyaged. Along these lines, the projectile can possibly ionize or investigate a substantial space if the mass is less and voyage way is long. Henceforth, the relative vitality of the progression pioneer controls the investigation and abuse of the calculation. A vital property of projectile is forking, which enhances the terrible arrangement of the populace and in the event that it isn't so one of the channels at the forking point is illuminated to keep the populace measure. In this calculation, three sorts of projectile are acquainted with speak to the entire advance pioneer development. These are progress projectile which develop the number of inhabitants in initial step pioneer, space projectile which endeavors to accomplish the best position and lead projectile which speaks to the best position among all populace. Since the change projectile are launched out an arbitrary way, it very well may be spoken to by an irregular number from uniform likelihood appropriation work, which is given by (13)

$$f(x^T) = \begin{cases} \frac{1}{b-a}; & a \le x^T \le b \\ 0 \quad ; & x < a, x^T > b \end{cases} \quad (13)$$

Where x^T is the irregular number that gives the arrangement or the underlying tip vitality of step pioneer *i*, *a* and *b* are the lower and upper limits of the arrangement space. In the wake of advancing the *N* step pioneer tips, it will move by ionizing the encompassing zone of the old pioneer utilizing vivacious projectiles in the subsequent stage. The situation of the space projectiles can be gotten from probability density function of exponential distribution as shown in (14)

$$f(x^s) = \begin{cases} \frac{1}{\mu} e^{-x^{si\mu}}; & a < x^T < b \\ 0 \quad ; & x^s \le 0 \end{cases} \quad (14)$$

where μ is the forming parameter which decides the space projectile position or bearing in the following stage. For a specific space projectile, μ_i is considered as the separation between a lead projectile and space projectile in the calculation. The situation of a specific space projectile is given by (15)

$$P^s_{i-new} = P^s_i \mp \exp\ rand_i\,(\mu_i) \quad (15)$$

In the event that the projectile vitality isn't more prominent than the progression pioneer, the new position of the space projectile does not guarantee engendering of the ventured pioneer to extend the channel. In the event that it isn't along these lines, it will move toward becoming lead projectile. The typical likelihood appropriation capacity of the lead projectile with scale parameter σ is given by (16)

$$f(x^L) = \frac{1}{\sigma\sqrt{2\pi}} e^{-(x^L-\mu)^2/2\sigma^2} \quad (16)$$

In LSA, the best solution can be obtained as shape parameter for space projectile and scale parameter decreases exponentially. The position of lead projectile is expressed in (17).

$$P^L_{new} = P^L + norm\ rand_i(\mu_L, \sigma_L) \quad (17)$$

On the off chance that the new position of the lead projectile gives a decent arrangement, at that point the progression pioneer is broadened and the lead projectile position is refreshed. Accordingly, the abuse and investigation are performed by space and lead projectiles to locate the ideal arrangement. The investigation is spoken to by the exponential arbitrary conduct of the space projectile and misuse process is controlled by the lead projectile with the irregular inquiry. The control parameters of LSA are populace estimate, most extreme emphasis and channel time. In this paper, populace measure, greatest emphasis and channel time are considered as 100, 100 and 20, individually.

IV. MATHEMATICAL MODELING OF VANADIUM REDOX FLOW BATTERIES UNIT

Electrochemical flow cell frameworks, otherwise called Vanadium Redox flow batteries (VRFB), convert electrical energy into compound potential energy by methods for a reversible electrochemical response between two fluid electrolyte arrangements. Interestingly with regular batteries, Redox flow cells store energy in the electrolyte arrangements. In this manner, the power and energy appraisals are free, with the capacity limit controlled by the amount of electrolyte utilized and the power rating dictated by the dynamic territory of the cell stack. The VRFB are fused in the power framework to meet the AGC issues and

 DOI : 10.18231/2454-9150.2019.0134

to guarantee an enhanced power quality. Specifically, these are fundamental for load leveling like breeze control and photovoltaic creating units, which require measures for ingestion of changes in output and to control glimmer and transitory voltage drop. The VRFB are equipped for guaranteeing a quick reaction and along these lines, chasing because of a postponement accordingly does not happen. Therefore, the ACEi was utilized straightforwardly as the direction esteem for LFC to control the output of VRFB. The block diagram representation of VRFB unit is shown in Fig 5. The Area Control Error (ACE) can be utilized as the control signal to the VRFB unit

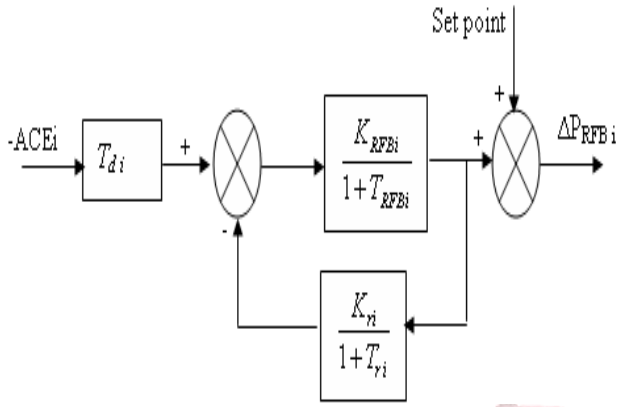

Fig. 5 Vanadium Redox Flow Battery System model

V. SIMULATION RESULTS AND OBSERVATIONS

In this study two-area solar-thermal deregulated power system is pain staked for the investigation with different generation schedules. Each area consists of two Gencos units and two discos units. The model of the framework under investigation has been created in MATLAB/SIMULINK condition. The ostensible parameters are given in Appendix. In this study, Lightning Search Algorithm (LSA) technique is utilized for ideal tuning FOPID controller for AGC loop of a two-area solar-thermal deregulated power with reheat bicycle mix condensation turbine. The ideal arrangement of control inputs is taken for improvement issue and the target work in Eqn (9) is determined to utilize the frequency deviations of control areas and tie-line power changes. The dynamic power model of VRFB unit is introduced in area1 to analyze its impact on the power system performance. The ideal FOPID controller gain estimations of test system without and with VRFB unit for different contextual analyses are recorded in the Table1 and 2. These FOPID controllers are executed in a proposed test system for various types of transactions with various generations schedules and contrasted and PI and PID controllers. The dynamic model steam turbine parameters have been utilized AGC loop under changing generation schedule condition.

Scenario 1: Poolco based transaction

In this situation, Gencos take an interest just in the load following control of their area.. It is accepted that a large step load 0.15 p.u. MW is demanded by each Disco in area 1. Expect that an instance of Poolco based contracts among Dicos and accessible Gencos is reproduced in light of the accompanying Disco Participation Matrix (DPM) alluding to Eq (1) is considered as

$$DPM = \begin{bmatrix} 0.5 & 0.5 & 0.0 & 0.0 \\ 0.5 & 0.5 & 0.0 & 0.0 \\ 0.0 & 0.0 & 0.0 & 0.0 \\ 0.0 & 0.0 & 0.0 & 0.0 \end{bmatrix} \quad (18)$$

$Disco_1$ and $Disco_2$ request indistinguishably from their neighborhood Gencos, viz., $Genco_1$ and $Genco_2$. In this way, $cpf_{11} = cpf_{12} = 0.5$ and $cpf_{21} = cpf_{22} = 0.5$. It might happen that a Disco violates an agreement by requesting more power than that predetermined in the agreement and this abundance power isn't contracted to any of the Gencos. This uncontracted power must be provided by the Gencos in a similar area to the Disco. It is represented as a local load of the area but not as the contract demand. Consider scenario-1 again with a modification that Disco demands as given in Table 1 and 2. From the Fig 6, the overall system performance as far as settling times and peak over/under shoots are likewise enormously enhanced with proposed LSA optimized FOPID controller contrasted with PI and PID controller. Besides, the dynamic performance is enhanced with facilitated use of VRFB units.

Scenario 2: Bilateral transaction

Here every one of the Discos has the contract with the Gencos and the accompanying Disco Participation Matrix (DPM) alluding to Eq (1) is considered as

$$DPM = \begin{bmatrix} 0.1 & 0.0 & 0.2 & 0.5 \\ 0.4 & 0.4 & 0.2 & 0.0 \\ 0.3 & 0.0 & 0.3 & 0.3 \\ 0.2 & 0.6 & 0.3 & 0.2 \end{bmatrix} \quad (19)$$

For this situation, the $Disco_1$, $Disco_2$, $Disco_3$ and $Disco_4$, requests of 0.1 pu.MW for each from Gencos as characterized by cpf in the DPM and each Gencos takes an interest in AGC as characterized by the accompanying area participation factor $apf_{11} = apf_{12} = 0.5$ and $apf_{21} = apf_{22} = 0.5$. The ideal FOPID controller gain estimations of test system without and with VRFB unit for different contextual analyses are recorded in the Table1 and 2 (case 5-8). The Fig.7 shows the dynamic responses of the frequency deviations, and tie- line power deviations, for a two area solar-thermal system without and with VRFB units (case-5). From the Fig 7, it can be observed that the frequency deviations of each area and tie-line power oscillations have improved with use of VRFB unit. The restoration procedure with the VRFB ensures not only reliable operation but provides a good margin of stability compared with the test system without VRFB units.

 DOI : 10.18231/2454-9150.2019.0134

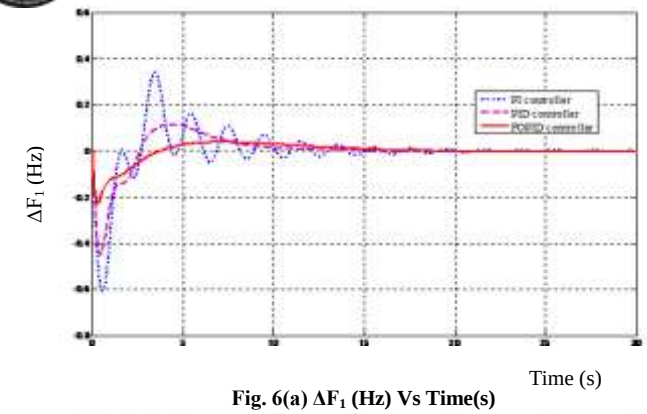

Fig. 6(a) ΔF_1 (Hz) Vs Time(s)

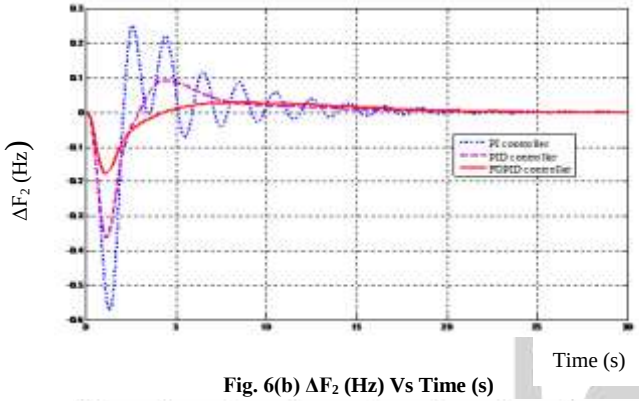

Fig. 6(b) ΔF_2 (Hz) Vs Time (s)

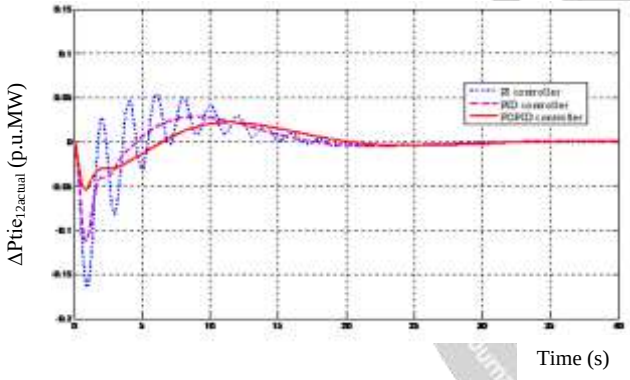

Fig. 6(c) $\Delta Ptie_{12,\ actual}$ (p.u.MW) Vs Time (s)

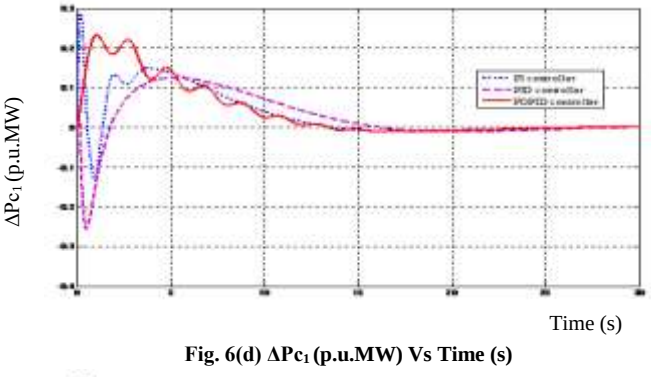

Fig. 6(d) ΔPc_1 (p.u.MW) Vs Time (s)

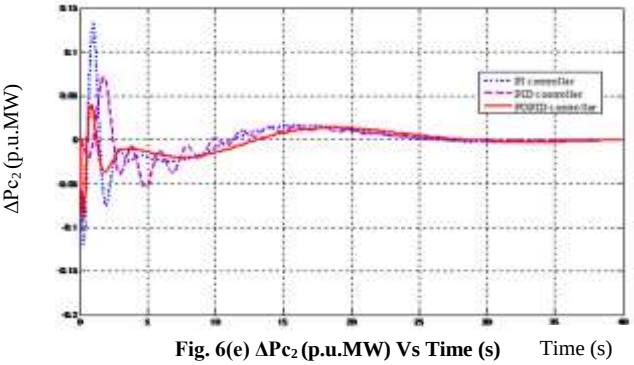

Fig. 6(e) ΔPc_2 (p.u.MW) Vs Time (s)

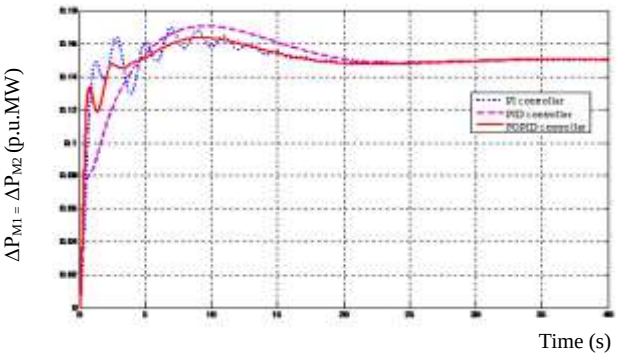

Fig. 6(f) ΔP_{M1}= ΔP_{M2} (p.u.MW) Vs Time (s)

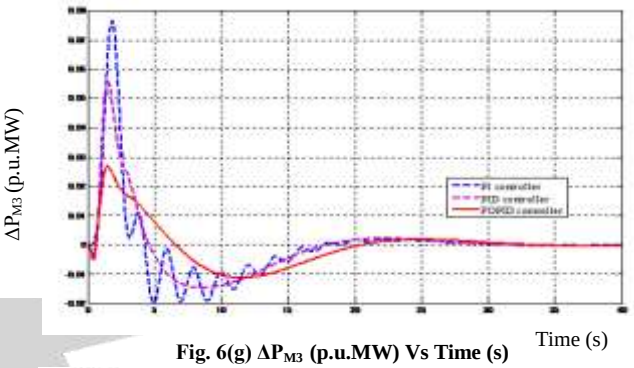

Fig. 6(g) ΔP_{M3} (p.u.MW) Vs Time (s)

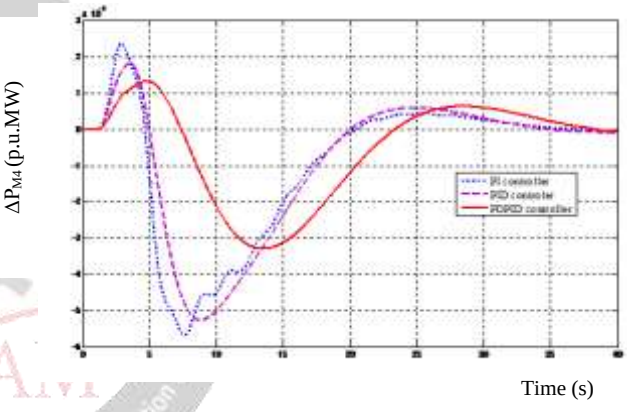

Fig. 6(h) ΔP_{M4} (p.u.MW) Vs Time (s)

Fig. 6 Dynamic responses of the frequency deviations, tie-line power deviations, Control input deviations and mechanical power generation deviations for a two area solar-thermal system using different types controllers (case-1)

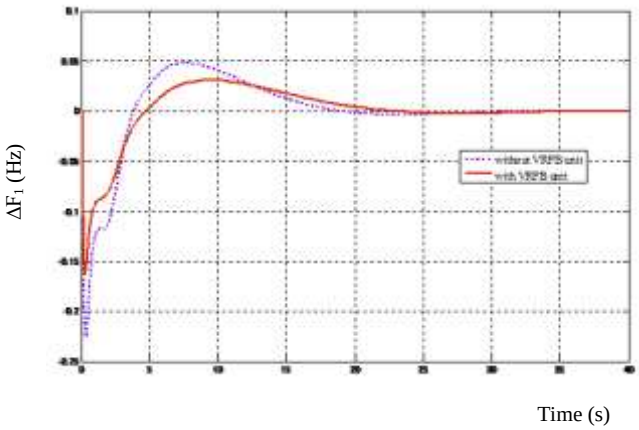

Fig. 7(a) ΔF_1 (Hz) Vs Time(s)

 DOI : 10.18231/2454-9150.2019.0134

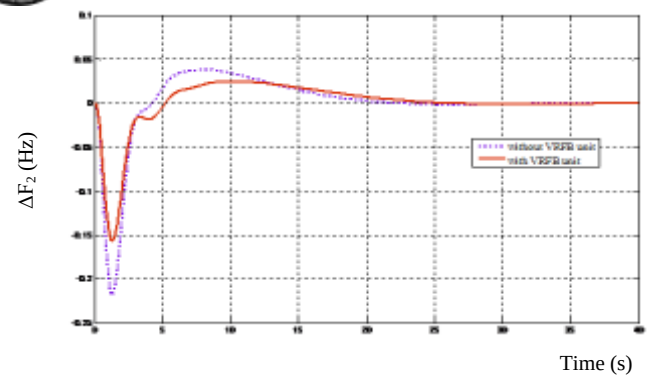

Fig. 7(b) ΔF_2 (Hz) Vs Time (s)

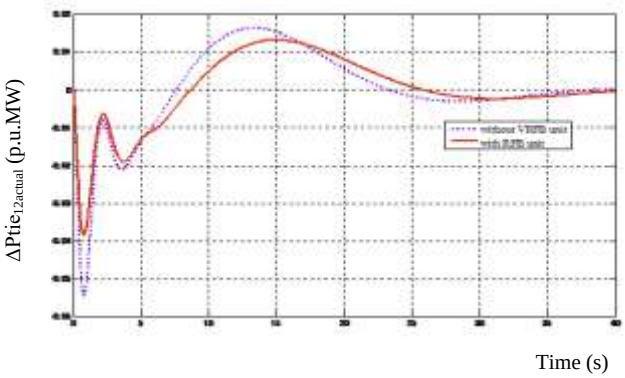

Fig. 7(c) $\Delta Ptie_{12,\ actual}$ (p.u.MW) Vs Time (s)

Fig.7 Dynamic responses of the frequency deviations, and tie- line power deviations, for a two area solar-thermal system without and with VRFB units

Table 1 Optimal FOPID controller gain values using LSA for two-area solar-thermal power system without VRFB unit for corresponding change in load demand

solar-thermal system	FOPID controller gain of area 1					FOPID controller gain of area 2					un contracted load demand pu.MW	
	K_{P1}	K_{I1}	K_{D1}	λ_1	μ_1	K_{P2}	K_{I2}	K_{D2}	λ_2	μ_2	area1	area2
Case 1	0.543	0.602	0.942	0.879	0.568	0.447	0.568	0.616	0.976	0.645	0.0	0.0
Case 2	0.574	0.644	0.962	0.894	0.612	0.524	0.573	0.623	0.845	0.783	0.1	0.0
Case 3	0.557	0.588	0.985	0.912	0.645	0.559	0.588	0.703	0.674	0.622	0.0	0.1
Case 4	0.594	0.756	0.989	0.945	0.655	0.653	0.743	0.615	0.744	0.734	0.1	0.1
Case 5	0.532	0.512	0.723	0.745	0.467	0.511	0.539	0.596	0.758	0.578	0.0	0.0
Case 6	0.548	0.534	0.812	0.644	0.643	0.523	0.545	0.602	0.796	0.743	0.05	0.0
Case 7	0.561	0.512	0.734	0.784	0.745	0.682	0.622	0.743	0.845	0.459	0.0	0.05
Case 8	0.573	0.581	0.878	0.458	0.848	0.711	0.744	0.886	0.764	0.571	0.05	0.05
Case 9	0.588	0.637	0.981	0.674	0.837	0.743	0.852	0.973	0.849	0.602	0.0	0.0
Case 10	0.643	0.751	0.989	0.864	0.945	0.755	0.863	0.982	0.748	0.457	0.05	0.0
Case 11	0.553	0.764	0.945	0.647	0.841	0.813	0.875	0.973	0.569	0.648	0.0	0.05
Case 12	0.571	0.867	0.949	0.974	0.901	0.846	0.843	0.986	0.642	0.773	0.05	0.05

Table 2 Optimal FOPID controller gain values using LSA for two-area solar-thermal power system with VRFB unit for corresponding change in load demand

solar-thermal system	FOPID controller gain of area 1					FOPID controller gain of area 2					un contracted load demand pu.MW	
	K_{P1}	K_{I1}	K_{D1}	λ_1	μ_1	K_{P2}	K_{I2}	K_{D2}	λ_2	μ_2	area1	area2
Case 1	0.438	0.511	0.847	0.785	0.463	0.312	0.459	0.537	0.871	0.548	0.0	0.0
Case 2	0.453	0.538	0.863	0.763	0.515	0.417	0.483	0.544	0.743	0.686	0.1	0.0
Case 3	0.442	0.475	0.888	0.824	0.567	0.443	0.491	0.619	0.574	0.552	0.0	0.1
Case 4	0.471	0.663	0.892	0.839	0.594	0.544	0.567	0.527	0.648	0.674	0.1	0.1
Case 5	0.429	0.427	0.635	0.643	0.363	0.409	0.443	0.467	0.659	0.472	0.0	0.0
Case 6	0.443	0.428	0.713	0.573	0.467	0.417	0.448	0.527	0.691	0.644	0.05	0.0
Case 7	0.457	0.409	0.634	0.664	0.559	0.586	0.527	0.635	0.744	0.557	0.0	0.05
Case 8	0.467	0.475	0.758	0.563	0.673	0.613	0.646	0.773	0.666	0.476	0.05	0.05
Case 9	0.483	0.532	0.845	0.558	0.642	0.663	0.743	0.883	0.747	0.508	0.0	0.0
Case 10	0.534	0.649	0.873	0.753	0.751	0.645	0.771	0.875	0.645	0.361	0.05	0.0
Case 11	0.448	0.657	0.835	0.537	0.653	0.763	0.784	0.883	0.664	0.563	0.0	0.05
Case 12	0.463	0.762	0.833	0.778	0.737	0.783	0.789	0.891	0.545	0.657	0.05	0.05

VI. CONCLUSION

The FOPID controllers are designed to utilize LSA strategy and acknowledged in two area solar-thermal interconnected power system without and with VRFB units for different types transactions. The various simulated results demonstrate that the proposed FOPID controller's execution is quick, more precise and superior to the reenacted results with PI and PID controllers. In FOPID besides proportional (K_P), integral (K_I) and derivative (K_D) gains, the controller has two more parameters, integral order (λ) and derivative order (μ) as design specifications which provide greater flexibility in controller design. VRFB unit is incorporated into area1 so as to enhance the system performance. It is seen that in every one of the cases (poolco based, bilateral based and contract violation based) the deviation of frequency ends up zero in the enduring state with less setting time as a result of the organized use of VRFB units which guarantees the prime necessity of AGC. The investigation likewise uncovers that the LSA strategy is more precise, solid and proficient in finding global optimal solution than other improvement algorithms.

 DOI : 10.18231/2454-9150.2019.0134

APPENDIX

A1 Control area and Gencos parameters (solar-thermal generating unit) and parameter of RFB unit [9, 19, 20]

Parameters	Area1	Area 2
Area capacities	1000 MW	1000 MW
Rating of single generating machine	500 MW	500 MW
Kp (Hz/p.u.MW)	120	120
Tp (sec)	20	20
B (p.u.MW / Hz)	0.425	0.425
R (Hz / p.u.MW)	$R_1=R_2=2.4$	$R_3=R_4=2.4$
Tg (sec)	$T_{g1}=T_{g2}=0.08$	$T_{g3}=0.08$, $T_{gs}=0.1$
Solar power plant parameter	$T_{gs}=0.1$ s, $T_{ts}=3$ s, $K_s=1.8$, $T_s=1.8$s	
Synchronising coefficient (p.u.MW / Hz)	$2\pi T_{12}=0.545$	
System frequency (F) in Hz	60 Hz	
Area participation factor (apf)	$apf_{11}=apf_{12}=apf_{21}=apf_{22}= 0.5$	
Area capacity ratios	$a_{12} = -1$	
Time constant of VRFB unit	$T_{VRFB} = 0.01$ sec	
Gain constant constant of VRFB unit	$K_{VRFB} = 1.8$	

ACKNOWLEDGMENT

The authors wish to thank the authorities of Annamalai University, Annamalainagar, Tamilnadu, India for the facilities provided to prepare this paper.

REFERENCES

[1] Shankar, R.; Pradhan, S.R.; Chatterjee, K.; and Mandal, R. (2017). A comprehensive state of the art literature survey on LFC mechanism for power system. Renewable and Sustainable Energy Reviews, 76, 1185-1207.

[2] Elgerd, O.I. (2014). "Electric energy systems theory: an introduction". Tata McGraw Hill Education Pvt. Ltd, New Delhi, India.

[3] V. Donde, M.A. Pai, I.A. Hiskens, Simulation and optimization in an AGC system after deregulation, IEEE Transactions on Power System, 16 (3) (2010) 311-322.

[4] Pardeep Nain, K.P.Singh Parmar and A.K. Singh, "Automatic Generation Control of an Interconnected Power System Before and After Deregulation", International Journal of Computer Applications, Vol. 61, No.15, pp.11-16, 2013.

[5] Bevrani H, Ghosh A, Ledwich G. Renewable energy sources and frequency regulation: survey and new perspectives. IET Renew Power Gener 2010;4(5):438–57

[6] Wang Li, Huang Cheng-Ching. Dynamic stability analysis of a grid-connected solar-concentrated ocean thermal energy conversion system. IEEE Trans Sust Energy 2010;1(1):10–8.

[7] Yatin Sharma and Lalit Chandra Saikia, "Automatic generation control of a multi-area ST – Thermal power system using Grey Wolf Optimizer algorithm based classical controllers", International Journal of Electrical Power & Energy Systems, Vol.73, pp.853-862, 2015.

[8] Das Dulal Ch, Sinha N, Roy AK. GA based frequency controller for solar thermal–diesel–wind hybrid energy generation/energy storage system. Int J Electr Power Energy Syst 2012;43(1):262–79.

[9] Sasaki, T.; Kadoya, T.; and Enomoto, K. (2004). Study on load frequency control using redox flow batteries. IEEE Transactions on Power Systems, 19(1), 660-667

[10] Saikia, L.C.; and Sahu, S.K. (2013). Automatic generation control of a combined cycle gas turbine plant with classical controllers using firefly algorithm. International Journal of Electrical Power and Energy Systems, 53, 27-33.

[11] Sahu, R.K.; Panda, S.; and Padhan, S. (2014). Optimal gravitational search algorithm for automatic generation control of interconnected power systems. Ain Shams Engineering Journal, 5(3), 721-733.

[12] Wei, Y.H; Sun, Z. Y.; Hu, Y. S,; and Wang, Y. (2015). On fractional order adaptive observer. International Journal of Automation and Computing. 12(6), 664–670.

[13] Swati, S; Yogesh, V.H. (2014). Fractional order PID controller for load frequency control. Energy Conversion and Management, 85, 343–353.

[14] Bhatt, P.; Roy, R.; and Ghoshal, S.P. (2010). GA/particle swarm intelligence based optimization of two specific varieties of controller devices applied to two-area multi-units automatic generation control. International journal of electrical power and energy systems, 32(4), pp.299-310.

[15] Nanda, J.; Mishra, S.; and Saikia, L.C. (2009). Maiden application of bacterial foraging-based optimization technique in multi area automatic generation control. IEEE Transactions on power systems, 24(2), 602-609.

[16] Chandrasekar, K.; Paramasivam, B.; and Chidambaram, I.A. (2017). Evaluation of power system restoration indices using krill herd algorithm based optimized pi+ controller for a restructured power system with facts devices. ARPN Journal of Engineering and Applied Sciences, 12, 4973-4989.

[17] Chatterjee, S.; and Mukherjee, V. (2016). PID controller for automatic voltage regulator using teaching–learning based optimization technique. International Journal of Electrical Power and Energy Systems, 77, 418-429.

[18] Shareef, H.; Ibrahim, A.A.; and Mutlag, A.H. (2015). Lightning search algorithm. Applied Soft Computing, 36, 315-333.

[19] Rajbongshi, R.; and Saikia, L.C. (2017). Combined control of voltage and frequency of multi-area multisource system incorporating solar thermal power plant using LSA optimised classical controllers. IET Generation, Transmission & Distribution, 11(10), 2489-2498.

[20] Nikhil Pathak, Ashu Verma, and Terlochan Singh Bhatti, " Automatic generation control of thermal power system under varying steam turbine dynamic model parameters based on generation schedules of the plants", The Journal of Engineering, Vol.24, pp.1-13, 2016.

 DOI : 10.18231/2454-9150.2019.0134